# Dmrt2 promotes transition of endochondral bone formation by linking Sox9 and Runx2

**Koichiro Ono**

    Osaka University Graduate School of Dentistry   https://orcid.org/0000-0002-0573-1481

**Kenji Hata** ( ✉ hata@dent.osaka-u.ac.jp )

    Osaka University Graduate School of Dentistry

**Eriko Nakamura**

    Department of Molecular and Cellular Biochemistry, Osaka University Graduate School of Dentistry

**Shota Ishihara**

    Osaka University Graduate School of Dentistry

**Sachi Kobayashi**

    Osaka University Graduate School of Dentistry

**Masako Nakanishi**

    Osaka University Graduate School of Dentistry

**Michiko Yoshida**

    Osaka University Graduate School of Dentistry

**Yoshifumi Takahata**

    Osaka University

**Tomohiko Murakami**

    Osaka University Graduate School of Dentistry

**Seiichi Takenoshita**

    Fukushima Medical University

**Toshihisa Komori**

    Basic and Translational Research Center for Hard Tissue Disease, Nagasaki University Graduate School of Biomedical Sciences, Nagasaki 852-8588

**Riko Nishimura**

    Department of Molecular and Cellular Biochemistry, Osaka University Graduate School of Dentistry
    https://orcid.org/0000-0001-7279-8363

**Toshiyuki Yoneda**

    Osaka University Graduate School of Dentistry

---

**Article**

# Abstract

Endochondral bone formation is fundamental for skeletal development. During this process, chondrocytes undergo multiple steps of differentiation and coordinated transition from a proliferating to a hypertrophic stage, which is critical to advance skeletal development. Here, we identified the transcription factor *Dmrt2* (double-sex and mab-3 related transcription factor 2) as a Sox9-inducible gene that promotes chondrocyte hypertrophy in pre-hypertrophic chondrocytes. Epigenetic analysis further demonstrated that Sox9 regulates *Dmrt2* expression through an active enhancer located 18 kb upstream of the *Dmrt2* gene and that this enhancer's chromatin status is progressively activated through chondrocyte differentiation. *Dmrt2*-knockout mice exhibited a dwarf phenotype with delayed initiation of chondrocyte hypertrophy. Dmrt2 augmented hypertrophic chondrocyte gene expression including *Ihh* through physical and functional interaction with Runx2. Furthermore, Dmrt2 deficiency reduced Runx2-dependent *Ihh* expression. Our findings suggest that Dmrt2 is critical for sequential chondrocyte differentiation during endochondral bone formation and coordinates the transcriptional network between Sox9 and Runx2.

# Introduction

Endochondral bone formation is the fundamental process of skeletal development in vertebrates [1]. Most of the mammalian skeleton is formed through this process, and mutations affecting endochondral bone formation cause skeletal abnormalities including chondrodysplasia, characterized by dwarfism and craniofacial abnormalities. Thus, uncovering the mechanism of endochondral bone formation should shed light on the pathophysiology of genetic skeletal disorders.

Endochondral bone formation occurs by sequential steps of chondrocyte differentiation [2]. Chondrocytes first arise from mesenchymal cells derived from cranial neural crest cells, sclerotomes, and lateral plate mesoderm. These cells undergo mesenchymal cell condensation and differentiate into early-stage chondrocytes, including round and proliferating chondrocytes that produce abundant chondrocyte-specific extracellular matrix proteins such as collagen type II alpha 1 chain (Col2a1) and Aggrecan (Acan) [2]. Proliferating chondrocytes then stop proliferating and enlarge their cell size to become pre-hypertrophic and hypertrophic chondrocytes [3], which are characterized by the expression of *Indian hedgehog* (*Ihh*) and *collagen type X alpha 1 chain* (*Col10a1*), respectively [4, 5]. These late-stage chondrocytes then undergo terminal differentiation and produce matrix metalloproteinase 13 (MMP13), which allows vascular invasion into cartilage [6]. Finally, terminal chondrocytes become apoptotic and are replaced by bone [2]. The sequential processes of early, late, and terminal chondrocyte differentiation construct a well-arranged columnar layer of chondrocytes called growth plate chondrocytes.

The function of stage-specific chondrocytes is strictly controlled by critical transcription factors [7−9]. In particular, Sry-related HMG-Box gene 9 (Sox9) plays indispensable roles in chondrocyte development and endochondral bone formation [10], and runt related transcription factor 2 (Runx2) and Runx3 play essential

roles in chondrocyte hypertrophy by directly regulating *Ihh* expression [9]. Chondrocyte-specific Sox9-knockout mice display severe defects in skeletal development and abnormal craniofacial development [10, 11] and double-knockout mice of Runx2 and Runx3 show the complete absence of hypertrophic chondrocytes [9]. Importantly, Sox9 regulates early-chondrocyte gene expressions, *Col2a1* and *Acan*, in collaboration with Sox5 and Sox6 [12]. Recent genome-wide analyses further demonstrated the genome-wide cooperation of Sox5/6/9 through super-enhancers of chondrocyte genes [12–14]. Because Sox9 expression initiates and promotes *Sox5* and *Sox6* expression [10], Sox5 and Sox6 are not essential for initiation of chondrogenesis but required for promotion of Sox9-regulated chondrogenesis.

Although it has long been accepted that Sox9 regulates early chondrogenesis, recent studies established that Sox9 is important for chondrocyte hypertrophy. Sox9, in association with myocyte enhancer factor 2C (Mef2c) and AP-1 family members, directly activates *Col10a1* expression to promote chondrocyte hypertrophy [15, 16]. Moreover, Sox9 is expressed in upper hypertrophic chondrocytes and maintains *Runx2* expression [15]. These reports strongly indicate that Sox9 target genes are also involved in chondrocyte hypertrophy and unknown molecules mediate the transition from proliferating to hypertrophic chondrocytes and conduct transcriptional machinery of the Sox9-Runx2 axis. However, in contrast to the wealth of knowledge regarding the Sox9 target genes in early chondrogenesis, the roles of Sox9 target genes in chondrocyte hypertrophy remain poorly understood. Thus, uncovering the target genes of Sox9 and their functional roles in chondrocyte hypertrophy would deepen our understanding of endochondral bone formation.

In this study, we discovered that Dmrt2 coordinates endochondral bone formation as a molecule downstream of Sox9. Sox9 and its partners Sox5 and Sox6 increased *Drmt2* gene expression along with chondrocyte differentiation. *Drmt2*-deficient mice showed the dwarf phenotype and delayed endochondral bone formation. Mechanistically, Dmrt2 promoted *Ihh* expression and chondrocyte hypertrophy through physical and functional collaboration with Runx2. Epigenetic analysis further revealed that Sox9 directly bound to H3K27ac positive enhancer located 18 kb upstream of the *Dmrt2* transcriptional start site (TSS) and that the chromatin status of this enhancer became progressively more active through chondrocyte differentiation. Thus, our findings provide novel insights into the transcription network controlling endochondral bone formation.

# Results

## Dmrt2 is a target gene of Sox5/6/9 in primary chondrocytes

To uncover the transcription factors involved in chondrocyte differentiation, we attempted to identify genes induced by Sox9 and its transcriptional cofactors, Sox5 and Sox6 (Sox5/6/9), in primary chondrocytes by performing RNA-seq based-cloning approach (Figure 1a). RNA-seq analysis with three biological replicates identified 1295 downregulated and 1209 upregulated genes using thresholds of false discovery rate (FDR) < 0.05 and fold change > 2 (Figure 1b). Relative to the levels in the control,

primary chondrocytes overexpressing Sox5/6/9 exhibited the upregulation of many known Sox9 target genes, including *Col2a1, Col11a1, Acan*, and *Matn1* (Figure 1c). Enrichment analysis of GO molecular function revealed 66 DNA-binding transcription factors upregulated by Sox5/6/9 (Figure 1d and Supplementary Table 1). Among these Sox5/6/9 target transcription factors, we were intrigued by the transcription factor Dmrt2. Although severe skeletal defects associated with *DMRT2* mutations have been reported in humans and mice [17-19], little is known about the functional roles of Dmrt2 in endochondral ossification. RT-qPCR confirmed that Sox5/6/9 upregulated *Col2a1* and *Dmrt2* expression in newborn rib chondrocytes, limb bud mesenchyme, and C3H10T1/2 cells (Figure 1e–g). Additionally, among the seven *Dmrt* family transcription factors, only *Dmrt2* showed strong expression in the rib cartilage of newborn mice (Supplementary Figure 1a), as well as Sox5/6/9-dependent induction in differentiating C3H10T1/2 cells (Supplementary Figure 1b). Collectively, these findings suggest that the collaboration of Sox5, Sox6, and Sox9 induces the expression of *Dmrt2* in chondrocytes.

## Dmrt2 is expressed in chondrocytes during endochondral bone formation *in vivo*

To examine whether *Dmrt2* is expressed in chondrocytes during endochondral bone formation, we first determined tissue distribution of Dmrt2 by perfuming RT-qPCR. We observed relatively high expression of *Dmrt2*, as well as the Sox9 target gene *Col2a1*, in rib cartilage (Figure 2a). Additionally, *Dmrt2* expression increased during *in vitro* chondrocyte differentiation of ATDC5 cells in the presence of *insulin-transferrin-selenium* (ITS), monitored by Alcian blue staining and *Col2a1* expression (Figure 2b). Furthermore, immunofluorescence analysis of E15.5 mouse tibia sections revealed that Dmrt2 was highly expressed in pre-hypertrophic chondrocytes, but weakly expressed in proliferating or hypertrophic chondrocytes (Figure 2c). Taken together, these findings suggest the possibility that Dmrt2 plays stage-specific roles in pre-hypertrophic chondrocytes during endochondral bone formation.

## Epigenetic regulation of Dmrt2 in chondrocytes

 To investigate the molecular mechanism by which Sox5/6/9 regulates *Dmrt2* gene expression, we analyzed an epigenetic dataset of chondrocytes including ATAC-seq, which allows the genome-wide profiling of the open chromatin region [20], and a ChIP-seq dataset [21]. We performed combination analysis of ATAC-seq profiles of growth plate chondrocytes (GSE100585) and ChIP-seq profiles of rib chondrocytes for Sox9, H3K27ac, and IgG (GSE69108). As shown in Figure 3a, we found a strong peak of the open chromatin region (chr19:25,728,596–25,729,301) located 18 kb upstream of *Dmrt2* TSS (Figure 3a). It should be noted that this region extensively overlaps with the peak of ChIP-seq for Sox9 and H3K27ac, an active enhancer mark of transcription (Figure 3a). Consistent with the bioinformatics analyses, reporter assay indicated that Sox9 and Sox5/6/9 significantly upregulated the transcriptional activity on the enhancer region (Figure 3b). These findings suggest that Sox9 upregulates Dmrt2 expression through an 18 kb upstream Sox9-bound enhancer.

We next examined whether the chromatin status of this Sox9-bound enhancer changes during chondrocyte differentiation. To achieve this, we obtained ChIP-seq datasets of E12.5 limb buds for Sox9 (GSE73225) [22] and H3K27ac (GSE45456) [23], and compared them with that of mature chondrocytes isolated from newborn ribs [21]. We found that Sox9 occupancy and active enhancer mark (H3K27ac) were very weak in E12.5 limb buds compared with the levels in rib chondrocytes (Figure 3c). ChIP-qPCR analysis further demonstrated that the enrichment of H3K27ac in differentiated ATDC5 cells became significantly higher than that of undifferentiated ATDC5 cells (Figure 3d). Taken together, these findings suggest that Sox9 directly regulates Dmrt2 expression through epigenetic regulation of the active enhancer.

## Dmrt2 is critical for endochondral bone formation *in vivo*

We next tested whether Dmrt2 regulates endochondral bone formation *in vivo* by examining *Dmrt2*-deficient (*Dmrt2$^{/-}$*) mice. *Dmrt2$^{-/-}$* mice died soon after birth, as reported previously [18]. Newborn *Dmrt2$^{-/-}$* mice showed a dwarf phenotype in contrast to wild-type (WT) and *Dmrt2* heterozygous mice, as determined by skeletal preparations and microcomputed tomography (microCT) analysis (Supplementary Figure 2a and 2b). Additionally, *Dmrt2$^{-/-}$* mice exhibited significantly shorter tibiae than WT mice (Figure 4a and 4b) and severely disrupted rib development, characterized by disorganized rib fusion and abnormal ossification in the sternum (Supplementary Figure 2c). In contrast, abnormal skeletal patterning was not observed in the hind paws of *Dmrt2$^{-/-}$* mice (Supplementary Figure 2d).

To investigate the potential role of Drmt2 in chondrocyte differentiation *in vivo*, we evaluated the organization of growth plate chondrocytes in newborn mice. Immunofluorescence analysis revealed disorganized Col2-positive and Col10-positive chondrocytes in the sternum of *Dmrt2$^{-/-}$* mice relative to the pattern in WT mice (Supplementary Figure 2e). Col2-positive rib cartilage of *Dmrt2$^{-/-}$* mice showed truncation, fusion, and bifurcation, and the Col10-positive hypertrophic chondrocyte zone in *Dmrt2$^{-/-}$* mice was shortened relative to that in WT mice (Supplementary Figure 2f).

To determine whether impaired endochondral bone formation might arise from suppressed chondrocyte proliferation in *Dmrt2$^{-/-}$* mice, we performed BrdU labeling assays of embryos. We found that the chondrocyte proliferation rate was not significantly reduced in *Dmrt2$^{-/-}$* mice relative to the level in WT mice (Figure 4c and 4d). Whole-mount *in situ* hybridization of WT and *Dmrt2$^{-/-}$* E13.5 embryos did not show significant differences in *Col2a1*- and *Sox9*-positive chondrocytes (Figure 4e), consistent with our findings that *Drmt2* is not yet expressed at this stage. These findings suggest that aberrant chondrocyte differentiation at a later stage, not proliferation, likely contributes to the skeletal abnormalities in *Dmrt2$^{-/-}$* mice.

We further examined how the loss of *Dmrt2* in mice affects the chondrocyte differentiation program during endochondral bone formation. At E14.5, WT embryos normally exhibited *Ihh*- and *Col10a1*-positive

chondrocytes in the tibial growth plate, but $Dmrt2^{-/-}$ embryos showed weak $Ihh$ expression and lacked $Col10a1$-positive chondrocytes (Figure 5a). At E15.0, the $Col2a1$-positive chondrocyte zone in WT embryos was completely divided by $Ihh$- and $Col10a1$-positive chondrocytes (Figure 5b), whereas $Col2a1$-positive chondrocytes in $Dmrt2^{-/-}$ embryos still existed among $Col10a1$-positive chondrocytes, and $Ihh$ and $Col10a1$ were weakly expressed (Figure 5b). Next, we quantitatively assessed $in situ$ hybridization sections to measure the lengths of the $Col2a1$ expressing zone (resting and proliferating chondrocyte zone), $Ihh$ expressing zone (pre-hypertrophic chondrocyte zone) and $Col10a1$ expressing zone (hypertrophic zone) in the tibiae of E15.0 mice (Figure 5c). We did not observe significant differences in the lengths of resting-proliferating zone between WT and $Dmrt2^{-/-}$ embryos (Figure 5c). However, the $Ihh$-positive pre-hypertrophic and $Col10a1$-positive hypertrophic zones were significantly shorter in $Dmrt2^{-/-}$ embryos than in WT embryos (Figure 5c). These findings suggest that impaired endochondral bone formation is partly responsible for the skeletal abnormalities in $Dmrt2^{-/-}$ mice.

### Dmrt2 promotes late chondrogenesis by functional interaction with Runx2

Given the delay in chondrocyte hypertrophy observed upon the loss of $Drmt2$, we determined whether Dmrt2 promotes the initiation of this process. Importantly, $Dmrt2$ overexpression in primary chondrocytes significantly upregulated the expression of $Ihh$ (Figure 6a). We noticed that the promoter of mouse $Ihh$, a specific marker of pre-hypertrophic chondrocytes, contains a consensus $Dmrt2$-binding element (BE, GnTACA) (Figure 6b). We found that Flag-tagged Dmrt2 bound to this element within the $Ihh$ gene promoter in primary chondrocytes as determined by ChIP assay (Figure 6c). A DNA-pulldown assay using a biotinylated Dmrt2-binding element also demonstrated that Dmrt2 directly bound to this element, and the Dmrt2 binding activity was decreased by a non-biotinylated probe in a dose-dependent manner (Figure 6d). These findings collectively suggest that Dmrt2 directly promotes $Ihh$ expression during endochondral bone formation.

 The transcription factor Runx2 directly regulates $Ihh$ expression, consequently stimulating chondrocyte hypertrophy [9]. We found that the Runx2 binding element in the $Ihh$ proximal promoter is located close to the Dmrt2 binding element (Figure 6b) and confirmed the direct binding of Runx2 to the Ihh gene promoter by ChIP assay (Figure 6e). Thus, we hypothesized that Dmrt2 functionally collaborates with Runx2 to regulate $Ihh$ expression. To prove this hypothesis, we ectopically expressed Dmrt2 and Runx2 in primary chondrocytes and examined $Ihh$ expression. Notably, primary chondrocytes overexpressing both Dmrt2 and Runx2 displayed higher $Ihh$ mRNA levels than cells overexpressing either Drmt2 or Runx2 alone, suggesting a synergistic interaction (Figure 6f). Dmrt2 and Runx2 also synergized to induce other Runx2 targets in primary chondrocytes, including $Alpl$ (alkaline phosphatase), $Col10a1$, and $Tcf7$ (Supplementary Figure 3). Further, coimmunoprecipitation experiments indicated physical association of Dmrt2 with Runx2 (Figure 6g). Venus-tagged Dmrt2 colocalized with DsRed-tagged Runx2 in the nucleus of C3H10T1/2 cells (Figure 6h), consistent with Dmrt2−Runx2 protein−protein interaction. Taken

together, these findings suggest that Dmrt2 interacts with and enhances Runx2 function at the target gene, *Ihh*.

## Impaired Runx2 function in *Dmrt2*^{-/-} chondrocytes

Finally, we examined whether the activities of Runx2 are affected in *Dmrt2*^{-/-} mice. To this end, we isolated primary chondrocytes from newborn WT and *Dmrt2*^{-/-} mice and examined the effect of Dmrt2 on Runx2 function by monitoring *Ihh* expression (Figure 7a).

WT and *Dmrt2*^{-/-} chondrocytes showed similar levels of endogenous Runx2 protein (Figure 7b) and we also found that loss of Dmrt2 did not affect the nuclear localization of endogenous Runx2 in primary chondrocytes, which suggests that Drmt2 does not affect the expression and stability of Runx2 (Figure 7c). Consistent with *ISH* analyses (Figure 5a and b), we found significantly reduced *Ihh* expression, the Runx2 target gene, in *Dmrt2*^{-/-} chondrocytes compared with the level in WT chondrocytes (Figure 7d). When we equally introduced Runx2 into primary chondrocytes isolated from WT and *Dmrt2*^{-/-} mice (Figure 7e), overexpression of Runx2 induced *Ihh* expression in WT chondrocytes, but this effect of Runx2 was reduced in *Dmrt2*^{-/-} chondrocytes (Figure 7f). These findings support the importance of interaction of Dmrt2 with Runx2 in *Ihh* expression.

# Discussion

Endochondral bone formation is achieved through successive chondrocyte differentiation steps that are strictly regulated in a spatiotemporal manner by various transcription factors. Previous biochemical and mouse genetic studies have shown that Sox9 regulates multiple steps of chondrocyte differentiation including early chondrogenesis and chondrocyte hypertrophy [15, 16]. Although the mechanisms by which Sox9 and its target genes regulate early chondrogenesis have been well studied, Sox9 target genes and their functional roles in chondrocyte hypertrophy remain poorly understood. In the present study, we discovered that the transcription factor Dmrt2 is selectively expressed in pre-hypertrophic chondrocytes and is induced by Sox5/6/9. We also found that Dmrt2 contributes to endochondral bone formation by promoting Runx2 functions. Our results suggest that Dmrt2 coordinates successive chondrocyte differentiation processes during skeletal development.

We identified Dmrt2 as a transcription factor functioning downstream of Sox5/6/9 in primary chondrocytes. Several studies have reported the targets of Sox9 or Sox5/6/9 in chondrocytes, but these targets promote early chondrogenesis and negatively regulate chondrocyte hypertrophy [24, 25]. Yamashita et al. reported that Bapx1, a direct target of Sox9, suppressed Runx2 activity in chondrocytes [25]. Additionally, Saito et al. found that S100A1 and S100B1 are directly regulated by Sox5/6/9 and they suppress chondrocyte hypertrophy and maturation [24]. We also identified the transcription factor Sp6 as a Sox9 target and showed that the deletion of Sp6 in mice results in a dwarf phenotype and impaired limb

development [26, 27]. These results fit the idea that Sox9 plays essential role in chondrogenesis. However, it is now established that Sox9 is required for chondrocyte hypertrophy [15, 16] and our findings suggest that target genes of Sox5/6/9 positively regulate chondrocyte hypertrophy. In addition to Dmrt2, FoxA2 and AP-1 family members, which were identified as Sox5/6/9-inducible genes (Supplemental Data 1), promote chondrocyte hypertrophy through functional interaction with Sox9 [16, 28]. Thus, other Sox5/6/9 target genes and their biological interaction with hypertrophic transcription factors warrant further investigation.

We found that Sox9 directly bound to the enhancer region of the *Dmrt2* gene located 18 kb upstream of its TSS by epigenetic analysis using ATAC-seq and ChIP-seq datasets. This region showed both open chromatin and H3K27ac, a histone mark for active enhancers (Fig. 3a). Ohba et al. previously reported that Sox9 has two distinct modes of action in chondrocytes [21]. Class I elements exist around the TSS of highly expressed genes not specific to chondrogenesis and Class II elements represent active enhancers that promote chondrocyte gene expression through the direct binding of Sox9. Intriguingly, a Sox9-occupied region located 18 kb upstream of Dmrt2 TSS belongs to Class II Sox9 binding elements [21], which suggests that Dmrt2 is the chondrocyte-specific Sox9 target gene in chondrocytes.

Although the ChIP-seq dataset and reporter assay demonstrated that Sox9 is responsible for the 18 kb upstream enhancer of the Dmrt2 gene, Sox9 alone failed to increase Dmrt2 expression in primary chondrocytes, limb bud mesenchyme, and C3H10T1/2 cells (Fig. 1e-g). We propose several possibilities to explain this. First, appropriate amounts of Sox5 and Sox6 are necessary to induce the transcription of Dmrt2. Previous studies have shown that Sox5 and Sox6 secure the DNA binding activity of Sox9 and cooperatively promote chondrocyte gene expression through super-enhancers at the genome-wide level [14, 29]. Liu et al. also reported that Sox6 and Sox9 bind genomic regions in the vicinity of each other [14]. It would be interesting to examine whether Sox6 binds a genomic region located close to the Sox9 binding region 18 kb upstream of Dmrt2 TSS. Second, an unknown epigenetic mechanism controlled by Sox5 and Sox6 is necessary for induction of the Dmrt2 gene. Many histone modification enzymes including demethylases and acetyltransferases are necessary for activating transcription in chondrocytes. Previous biochemical and epigenetic studies showed that Sox9 functionally interacts with CBP/P300, which works as a histone acetyltransferase [21, 30]. Our group has shown that the histone demethylase PHF2 associates with Sox9 to promote Sox9 target gene expression in chondrocytes [31]. Although we did not provide direct evidence showing that Sox5 and Sox6 control histone modification, it is likely that they upregulate Dmrt2 expression through epigenetic remodeling. More studies are necessary to uncover the precise molecular mechanism underlying the effects of Sox5 and Sox6 to activate Dmrt2 gene expression in chondrocytes.

Because Sox5/6/9 increase *Dmrt2* mRNA and are strongly expressed in resting and proliferating chondrocytes, we first predicted that Dmrt2 is widely expressed in resting and proliferating chondrocytes. Unexpectedly, immunohistochemical analysis revealed that Dmrt2 protein is selectively expressed in pre-hypertrophic chondrocytes (Fig. 2c). These findings raise the possibility that other unknown transcription factors that are selectively expressed in pre-hypertrophic chondrocytes are required to accelerate Dmrt2

expression. Alternatively, post-transcriptional regulation of Dmrt2 controls pre-hypertrophic specific protein expression. This complexity found to be exhibited for many genes expressed in chondrocytes of the growth plate. For instance, Ihh expression is known to be limited to pre-hypertrophic chondrocytes, but Runx2, which directly regulates Ihh, is widely expressed in both pre-hypertrophic and hypertrophic chondrocytes [9, 32]. Additionally, PTHrP is only detectable in the periarticular region, even though the Gli family, signaling molecules of Ihh, are diffusely distributed in round and proliferating chondrocytes [5, 33]. The molecular mechanisms that control the specific expression of chondrocyte genes are not fully understood, so further studies are necessary to clarify these.

Dmrt2 contains a highly conserved DNA binding domain called the DM domain, but its sequence similarity with other Dmrt family members is low outside the DM domain [34]. The DM domain recognizes a consensus sequence and physically interacts with DNA in the minor groove [35]. Dmrt proteins are predicted to bind DNA as heterodimers or homodimers with other Dmrt family proteins [36]. Importantly, Dmrt proteins act as bifunctional transcriptional regulators to activate or repress transcription [34]. For instance, Dmrt1 inhibits Stra8 but activates Sohlh1 in germ cells, which prevents meiosis and promotes spermatogonial development [37]. Whether Dmrt1 activates or represses transcription appears to depend on motifs around Dmrt1 binding sites, which suggests that the function of Dmrt1 depends on co-activators and co-repressors [38]. These findings raise the possibility that Dmrt2 also exerts a reciprocal function in chondrocytes in addition to the increase of Runx2 function. Notably, pre-hypertrophic chondrocytes are the transition stage from a proliferating to a hypertrophic state, at which the expression of proliferating chondrocyte-specific genes such as *Col2a1* and *Aggrecan* should be inhibited at the transcriptional level. It would be interesting to determine whether Dmrt2 controls chondrocyte differentiation by suppressing Sox9-dependent gene expression but promoting Runx2-dependent gene expression in pre-hypertrophic chondrocytes. The regulation of Sox9 function by Dmrt2 during endochondral bone formation awaits further investigation.

In conclusion, our work suggests a novel role for Dmrt2 during endochondral bone formation as a transcriptional coactivator of Runx2. These findings increase our understanding of the molecular mechanisms of endochondral bone formation and provide new insights into the transcription factor network controlling skeletal development.

# Methods

## Cell culture and reagents

The mouse fibroblast-like cell line C3H10T1/2 and mouse teratocarcinoma cell line ATDC5 were purchased from the RIKEN Cell Bank (Ibaraki, Japan). These cells were cultured at 37°C in a humidified 5% $CO_2$ incubator with Dulbecco's modified Eagle's medium (DMEM; Sigma-Aldrich, St. Louis, MO, USA) containing 10% fetal bovine serum (FBS) and a 1:1 mixture of DMEM and Ham's F-12 medium (Sigma-Aldrich) containing 10% FBS. Insulin-transferrin-sodium selenite supplement (ITS; Roche, Basel,

Switzerland) was used to induce chondrocyte differentiation in ATDC5 cells. Primary chondrocytes were isolated in accordance with a protocol described by Gartland et al. [39]. Briefly, rib cartilage was dissected from newborn mice and soft tissue was removed. Then, rib cartilage was digested with 0.1% collagenase D (Roche) and 0.5% trypsin (Life Technology, Carlsbad, CA, USA) for 6 h at 37°C. Primary chondrocytes were collected by centrifugation and resuspended with DMEM containing 10% FBS and antibiotics. Cells within two passages were used for experiments as primary chondrocytes.

## Generation of adenoviruses

cDNAs of Flag-tagged-Dmrt2, HA-tagged-Sox9, Sox5, Sox6, and Runx2 were amplified using Pfu DNA polymerase and subcloned into pAXCAwt vectors (TAKARA Bio, Shiga, Japan). Recombinant adenoviruses were generated using the COS-TPC method by transfection of a recombinant cosmid and the DNA-TPC adenovirus genome into 293 cells [31]. C3H10T1/2 cells, ATDC5 cells, and primary chondrocytes were infected with adenoviruses at a multiplicity of infection (MOI) of 20 unless indicated otherwise.

## RNA-seq

Total RNA was extracted from primary chondrocytes in which control vector or Sox5/6/9 were adenovirally expressed using NucleoSpin RNA II (Macherey-Nagle, Duren, Germany). Total RNA library preparation was performed using a TruSeq stranded mRNA sample prep kit (Illumina, San Diego, CA, USA), in accordance with the manufacturer's protocol. Sequencing was performed on an Illumina HiSeq 2500 platform in 75-base single-end mode. Illumina Casava1.8.2 software was used for base-calling. Sequenced reads were mapped to the mouse reference genome sequence (mm10) using TopHat v2.0.13 in combination with Bowtie2 ver. 2.2.3 and SAMtools ver. 0.1.19.

RNA-seq data were analyzed using iDEP (integrated Differential Expression and Pathway analysis) [40]. Briefly, read count data of three replicates for control and Sox5/6/9 were generated and uploaded to the iDEP website (http://bioinformatics.sdstate.edu/idep/). Differentially expressed genes (DEGs) were identified using a threshold of false discovery rate (FDR) < 0.05 and minimal fold change > 2. The raw data have been deposited in the NCBI Gene Expression Omnibus database (GEO GSE155118).

Reverse-transcription polymerase chain reaction (RT-PCR) and RT-qPCR

Total RNA was isolated using a Nucleo Spin RNA Plus kit. cDNA was synthesized using ReverTra Ace$^®$ qPCR RT Master Mix (TOYOBO, Osaka, Japan). For RT-PCR analysis, cDNA was amplified using KOD FX (TOYOBO) and then the PCR products were electrophoresed in a 1.6% agarose gel with ethidium bromide. Primer pairs used for RT-PCR analysis are listed in Supplemental Table S2. For RT-qPCR analysis, cDNA was amplified with EagleTaq Universal Master Mix (ROX) using a StepOnePlus Real-Time PCR System (Applied Biosystems, Foster City, CA, USA). Primers and TaqMan probes used for cDNA amplification are listed in Supplementary Table S2. The mRNA expression was normalized to β-actin expression levels.

## Epigenetic datasets and analysis

ChIP-seq and ATAC-seq datasets were downloaded from the GEO database. We obtained GSE69109 ChIP-seq profiles of newborn mouse rib chondrocytes for Sox9 and H3K27ac [21]. ChIP-seq profiles of E12.5 limb buds for Sox9 were obtained from GSE73225 [23] and H3K27ac from GSE45456 [22]. ATAC-seq datasets of growth plate chondrocytes were downloaded from GSE100585 [20].

FASTQ data of ChIP-seq and ATAC-seq were aligned to the mouse genome (mm10) using Bowtie and peak calling was performed using MACS software with the default settings (p-value cut-off = 1.00e-05). ChIP-seq and ATAC-seq data were visualized using the Integrative *Genomics Viewer* (*IGV*).

## Reporter assay

*Dmrt2* minimal promoter (−100 to +10) and Sox9 binding region located 18 kb upstream of the *Dmrt2* TSS were introduced upstream of the luciferase gene. Reporter genes were co-transfected with the expression vectors and *Renilla* into HEK293 cells using the FuGENE6 reagent. After 48 h of transfection, the cells were lysed and luciferase activity was measured using specific substrates in a luminometer (Promega, Fitchburg, WI, USA), in accordance with the manufacturer's protocol. Luciferase activity was normalized by *Renilla*.

## Mice

*Dmrt2*^{−/−} mice were originally generated by Dr. Randy L. Johnson (Department of Biochemistry and Molecular Biology, The University of Texas MD Anderson Cancer Center) [18]. They were maintained and kindly provided by Dr. David Zarkower (Developmental Biology Center and Department of Genetics, Cell Biology, and Development, University of Minnesota) for the experiments. To determine the genotypes of the mice, genomic DNA was purified from mouse tails and examined by PCR using KOD FX Neo (Toyobo). Primer pairs for genotyping were as follows: WT, sense 5'-CTGGACCCGAGTACAGTTCC-3' and antisense 5'-AATGGTGCGTTCAACTCAGG-3'; KO, sense 5'-TGCGGAGGGCTGGATCTTAAGGAG-3' and antisense 5'-AGGGGGTGGGGATTTGACACCATC-3'. The PCR product of WT mice was 830 bp and that of KO mice was 270 bp.

All mice were maintained on the C57BL/6 background. Littermate embryos were used for histological analysis. All animal experiments were performed using protocols approved by the Animal Committee of Osaka University Graduate School of Dentistry.

## Skeletal preparation

The skin of the mice was removed and fixed in 95% ethanol overnight. Cartilage tissues were stained with 1.5% Alcian blue followed by staining of bone tissues with 0.02% Alizarin red S. Skeletal samples were photographed under a stereoscopic microscope.

## Immunohistochemistry

Samples were fixed with 4% buffered paraformaldehyde, embedded in paraffin, and cut into 4-µm-thick sections. Paraffin-embedded sections were *deparaffinized* and rehydrated, followed by hematoxylin and eosin (H&E) staining. For immunohistochemical analysis, antigen retrieval was performed by incubation in DAKO REAL target retrieval solution for 10 min at 90°C, followed by blocking with 1% bovine serum albumin in phosphate-buffered saline (PBS). Immunohistochemistry was performed using the following antibodies: anti-Dmrt2 (#ARP32224_P050; AVIVA System Biology, CA, USA) at 5 µg/ml, anti-Col2 (#7050; Chondrex, WA, USA) at 1:500 (vol/vol) dilution, and anti-Col10 (LSL LB-0092; Cosmo Bio, Tokyo, Japan) at 1:500 (vol/vol) dilution. Immunoreactivity was visualized with Alexa Fluor® 555 dye-conjugated anti-rabbit IgG (Invitrogen, CA, USA), and counterstaining was performed using 4¢,6-diamidino-2-phenylindole, in accordance with the manufacturer's protocol.

## *In situ* hybridization

The protocol for *in situ* hybridization has been described in a previous report [41]. Briefly, tissues harvested from WT and *Dmrt2*−/− littermate mice were fixed with 4% paraformaldehyde and then embedded in paraffin. The tissue blocks were cut into 4-µm-thick sections. Digoxigenin (DIG)-11-UTP-labeled, single-stranded RNA probes were prepared using a DIG RNA labeling kit (Roche), in accordance with the manufacturer's instructions. We used a 0.4 kb fragment of mouse *Col2a1* cDNA, a 0.65 kb fragment of mouse *Col10a1* cDNA, and a 0.57 kb fragment of mouse *Ihh* cDNA to generate antisense and sense probes. Signals were detected with an alkaline phosphatase-conjugated anti-DIG antibody (Roche). All probes were kindly provided by Dr. Noriyuki Tsumaki (Kyoto University, Kyoto, Japan).

## BrdU assay

Pregnant mice were anesthetized and administered 1 ml of BrdU Labeling Reagent (Life Technologies) per 100 g body weight by intraperitoneal injection. The mice were sacrificed 2 h later, after which E17.5 WT and *Dmrt2*−/− littermate mouse tibiae were collected and fixed with 4% paraformaldehyde. Paraffin-embedded sections were subjected to a BrdU assay using a BrdU Staining kit (Invitrogen). For quantitative analysis, BrdU-positive nuclei in round and hypertrophic chondrocytes were excluded.

## Western blotting

Cells were rinsed twice with PBS and solubilized in lysis buffer [20 mM HEPES, pH 7.4, 150 mM NaCl, 1 mM EGTA, 1.5 mM $MgCl_2$, 10% glycerol, 1% Triton X-100, 10 µg/ml aprotinin, 10 µg/ml leupeptin, 1 mM 4-(2-aminoethyl) benzenesulfonyl fluoride hydrochloride, and 0.2 mM sodium orthovanadate]. The lysates were centrifuged at 4°C for 10 min at 15,000 × *g* and then boiled in sodium dodecyl sulfate (SDS) sample buffer containing 0.5 M β-mercaptoethanol for 5 min. The supernatant was separated by SDS-polyacrylamide gel electrophoresis, transferred to a nitrocellulose membrane, immunoblotted with a primary antibody, and then visualized with horseradish peroxidase-coupled anti-mouse or -rabbit IgGs using an enhanced chemiluminescence detection kit (Immunostar LD; WAKO, Osaka, Japan). An anti-Flag (M2) antibody was purchased from Sigma-Aldrich. Anti-HA (Y-11, #sc-805) was purchased from Santa

Cruz Biotechnology (CA, USA). Antibodies against β-actin (M177-3), and Runx2 (D1L7F) were purchased from MBL (Nagoya, Japan) and CST (MA, USA), respectively.

## Whole-mount *in situ* hybridization

DIG-labeled antisense RNA probes for Col2a1 and Sox9 were generated with SP6 or T7 RNA polymerase using the DIG RNA Labeling kit, in accordance with the manufacturer's instructions. Embryos of WT and *Dmrt2*$^{-/-}$ littermate mice at E13.5 were fixed in 4% paraformaldehyde/PBS overnight at 4°C. The samples were then hybridized overnight with gene-specific DIG-labeled RNA probes at 70°C overnight. Then, the samples were washed and incubated with an anti-DIG antibody (Antidigoxigenin-AP; Roche). Nitroblue tetrazolium and BCIP (5-bromo-4-chloro-3'-indolyphosphate p-toluidine) were used for signal detection.

## ChIP assays

ChIP analysis was performed using a ChIP-IT express kit (Active Motif), in accordance with the manufacturer's instructions. Briefly, primary chondrocytes and ATDC5 cells were washed with PBS, and chromatin was fixed with formaldehyde to crosslink the proteins to chromatin. Crosslinked chromatin was sonicated with Covaris M220. Sonicated chromatin was immunoprecipitated with an anti-H3K27ac antibody (D5E4, CST), anti-Flag (M2) antibody, and anti-Runx2 antibody (D1L7F, CST). DNA fragments were precipitated with protein-A magnetic beads and amplified by PCR using primer pairs specific for the Sox9-bound enhancer of the *Dmrt2* gene (sense primer, 5¢-TTCCAGATGGGCTGAAAC-3¢; anti-sense primer, 5¢-CTGTGCATTGTGGGAGAG-3¢), *Ihh* gene promoter containing the Dmrt2-binding element (sense primer, 5¢-TGGCCTTTCTCCCTTGTTTTT-3¢; anti-sense primer, 5¢-CAATGTAGCCTTGTCAGGAGTCA-3¢), and *Ihh* gene promoter containing the Runx2-binding element (sense primer, 5¢-**AGCTTTCGGGTTTGCTTCTC**-3¢; anti-sense primer, 5¢-**GTCTCTCCTTCCCGTTCCTT**-3¢). Quantitative analysis of ChIP assays was performed by real-time PCR using SYBR Green.

## DNA pulldown assays

Cells were lysed in lysis buffer (20 mM HEPES, pH 7.4, 150 mM NaCl, 1 mM EGTA, 1.5 mM MgCl$_2$, 10% glycerol, 1% Triton X-100, 10 µg/ml leupeptin, 1 mM PMSF, and 0.2 mM sodium orthovanadate). Lysates pre-incubated with streptavidin agarose beads were incubated with 1 µg of a biotinylated double-stranded oligonucleotide probe containing the Dmrt2-binding element in the *Ihh* gene promoter (sense primer, 5'-AAATAACCAAGATACAATTTGCAAAACACA-3'; anti-sense primer, 5'-TGTGTTTTGCAAATTGTATCTTGGTTATTT-3') for 3 h. Precipitated oligonucleotides were collected with streptavidin magnetic beads (Dynabeads My One Streptavidin T1, Invitrogen) and washed with lysis buffer. The magnetic beads were resuspended with SDS sample buffer, boiled for 5 min, and then subjected to western blotting.

## Statistical analysis

Randomization and *blinding* were not performed in the *animal studies.* Sample sizes were estimated based on previous studies of endochondral bone formation [31, 41]. Data were statistically analyzed by Student's *t*-test for comparison between two groups. For more than two groups, we used one-way analysis of variance (ANOVA) or two-way ANOVA followed by the Tukey test. At least five mice ($n$ = 5–6) were used for the phenotypic analysis. *P*-values of less than 0.05 were considered statistically significant.

# Declarations

## Acknowledgments

## Funding

## Author contributions

K.O. and K.H. designed and performed all *in vitro* and *in vivo* experiments. K.O., E.N., S.I., S.K., K.H., M.Y., T.M., and Y.T. performed the molecular and biochemical experiments. N.M. performed histological analyses. S.T., T.K., and T.Y. discussed and assessed the data. K.H. and R.N. directed the project and interpreted the data. All authors participated in writing of the manuscript

## Ethics

Animal experimentation was performed in strict accordance with the guidelines for proper conduct of animal experiments and related activities of Osaka University Graduate School of Dentistry. All of the

animals were handled in accordance with the protocol approved by the Animal Committee of Osaka University Graduate School of Dentistry.

## Data availability

RNA-seq data have been deposited in the NCBI Gene Expression Omnibus (https://www.ncbi.nlm.nih.gov/geo/) under accession number GSE155118.

## Competing interests

The authors declare no competing interests.

# References

1. Long, F. & Ornitz, D.M. Development of the endochondral skeleton. *Cold Spring Harbor perspectives in biology* **5**, a008334 (2013).
2. Kronenberg, H.M. Developmental regulation of the growth plate. *Nature* **423**, 332–336 (2003).
3. Sun, M.M. & Beier, F. Chondrocyte hypertrophy in skeletal development, growth, and disease. *Birth defects research. Part C, Embryo today: reviews* **102**, 74–82 (2014).
4. Kielty, C.M., Kwan, A.P., Holmes, D.F., Schor, S.L. & Grant, M.E. Type X collagen, a product of hypertrophic chondrocytes. *The Biochemical journal* **227**, 545–554 (1985).
5. Vortkamp, A. *et al.* Regulation of rate of cartilage differentiation by Indian hedgehog and PTH-related protein. *Science (New York, N.Y.)* **273**, 613–622 (1996).
6. Johansson, N. *et al.* Collagenase-3 (MMP-13) is expressed by hypertrophic chondrocytes, periosteal cells, and osteoblasts during human fetal bone development. *Developmental dynamics: an official publication of the American Association of Anatomists* **208**, 387–397 (1997).
7. Akiyama, H. & Lefebvre, V. Unraveling the transcriptional regulatory machinery in chondrogenesis. *Journal of bone and mineral metabolism* **29**, 390–395 (2011).
8. Liu, C.F., Samsa, W.E., Zhou, G. & Lefebvre, V. Transcriptional control of chondrocyte specification and differentiation. *Seminars in cell & developmental biology* (2016).
9. Yoshida, C.A. *et al.* Runx2 and Runx3 are essential for chondrocyte maturation, and Runx2 regulates limb growth through induction of Indian hedgehog. *Genes & development* **18**, 952–963 (2004).
10. Akiyama, H., Chaboissier, M.C., Martin, J.F., Schedl, A. & de Crombrugghe, B. The transcription factor Sox9 has essential roles in successive steps of the chondrocyte differentiation pathway and is required for expression of Sox5 and Sox6. *Genes & development* **16**, 2813–2828 (2002).

11. Mori-Akiyama, Y., Akiyama, H., Rowitch, D.H. & de Crombrugghe, B. Sox9 is required for determination of the chondrogenic cell lineage in the cranial neural crest. *Proceedings of the National Academy of Sciences of the United States of America* **100**, 9360–9365 (2003).

12. Lefebvre, V., Behringer, R.R. & de Crombrugghe, B. L-Sox5, Sox6 and Sox9 control essential steps of the chondrocyte differentiation pathway. *Osteoarthritis and cartilage* **9 Suppl A**, S69-75 (2001).

13. Lefebvre, V., Li, P. & de Crombrugghe, B. A new long form of Sox5 (L-Sox5), Sox6 and Sox9 are coexpressed in chondrogenesis and cooperatively activate the type II collagen gene. *EMBO J* **17**, 5718–5733 (1998).

14. Liu, C.F. & Lefebvre, V. The transcription factors SOX9 and SOX5/SOX6 cooperate genome-wide through super-enhancers to drive chondrogenesis. *Nucleic Acids Res* **43**, 8183–8203 (2015).

15. Dy, P. *et al.* Sox9 directs hypertrophic maturation and blocks osteoblast differentiation of growth plate chondrocytes. *Dev Cell* **22**, 597–609 (2012).

16. He, X., Ohba, S., Hojo, H. & McMahon, A.P. AP-1 family members act with Sox9 to promote chondrocyte hypertrophy. *Development* **143**, 3012–3023 (2016).

17. Bouman, A. *et al.* Homozygous DMRT2 variant associates with severe rib malformations in a newborn. *American journal of medical genetics. Part A* **176**, 1216–1221 (2018).

18. Seo, K.W. *et al.* Targeted disruption of the DM domain containing transcription factor Dmrt2 reveals an essential role in somite patterning. *Dev Biol* **290**, 200–210 (2006).

19. Ounap, K. *et al.* Three patients with 9p deletions including DMRT1 and DMRT2: a girl with XY complement, bilateral ovotestes, and extreme growth retardation, and two XX females with normal pubertal development. *American journal of medical genetics. Part A* **130A**, 415–423 (2004).

20. Guo, M. *et al.* Epigenetic profiling of growth plate chondrocytes sheds insight into regulatory genetic variation influencing height. *Elife* **6** (2017).

21. Ohba, S., He, X., Hojo, H. & McMahon, A.P. Distinct Transcriptional Programs Underlie Sox9 Regulation of the Mammalian Chondrocyte. *Cell reports* **12**, 229–243 (2015).

22. Andrey, G. *et al.* A switch between topological domains underlies HoxD genes collinearity in mouse limbs. *Science (New York, N.Y.)* **340**, 1234167 (2013).

23. Garside, V.C. *et al.* SOX9 modulates the expression of key transcription factors required for heart valve development. *Development* **142**, 4340–4350 (2015).

24. Saito, T., Ikeda, T., Nakamura, K., Chung, U.I. & Kawaguchi, H. S100A1 and S100B, transcriptional targets of SOX trio, inhibit terminal differentiation of chondrocytes. *EMBO Rep* **8**, 504–509 (2007).

25. Yamashita, S. *et al.* Sox9 directly promotes Bapx1 gene expression to repress Runx2 in chondrocytes. *Exp Cell Res* **315**, 2231–2240 (2009).

26. Nakamura, T. *et al.* Transcription factor epiprofin is essential for tooth morphogenesis by regulating epithelial cell fate and tooth number. *The Journal of biological chemistry* **283**, 4825–4833 (2008).

27. Talamillo, A. *et al.* Role of Epiprofin, a zinc-finger transcription factor, in limb development. *Dev Biol* **337**, 363–374 (2010).

28. Ionescu, A. *et al.* FoxA family members are crucial regulators of the hypertrophic chondrocyte differentiation program. *Dev Cell* **22**, 927–939 (2012).

29. Liu, C.F., Angelozzi, M., Haseeb, A. & Lefebvre, V. SOX9 is dispensable for the initiation of epigenetic remodeling and the activation of marker genes at the onset of chondrogenesis. *Development* **145** (2018).

30. Furumatsu, T. *et al.* Sox9 and p300 cooperatively regulate chromatin-mediated transcription. *The Journal of biological chemistry* **280**, 35203–35208 (2005).

31. Hata, K. *et al.* Arid5b facilitates chondrogenesis by recruiting the histone demethylase Phf2 to Sox9-regulated genes. *Nature communications* **4**, 2850 (2013).

32. Enomoto, H. *et al.* Cbfa1 is a positive regulatory factor in chondrocyte maturation. *The Journal of biological chemistry* **275**, 8695–8702 (2000).

33. Mau, E. *et al.* PTHrP regulates growth plate chondrocyte differentiation and proliferation in a Gli3 dependent manner utilizing hedgehog ligand dependent and independent mechanisms. *Dev Biol* **305**, 28–39 (2007).

34. Bellefroid, E.J. *et al.* Expanding roles for the evolutionarily conserved Dmrt sex transcriptional regulators during embryogenesis. *Cellular and molecular life sciences: CMLS* **70**, 3829–3845 (2013).

35. Narendra, U., Zhu, L., Li, B., Wilken, J. & Weiss, M.A. Sex-specific gene regulation. The Doublesex DM motif is a bipartite DNA-binding domain. *The Journal of biological chemistry* **277**, 43463–43473 (2002).

36. Murphy, M.W., Zarkower, D. & Bardwell, V.J. Vertebrate DM domain proteins bind similar DNA sequences and can heterodimerize on DNA. *BMC Mol Biol* **8**, 58 (2007).

37. Matson, C.K. *et al.* The mammalian doublesex homolog DMRT1 is a transcriptional gatekeeper that controls the mitosis versus meiosis decision in male germ cells. *Dev Cell* **19**, 612–624 (2010).

38. Murphy, M.W. *et al.* Genome-wide analysis of DNA binding and transcriptional regulation by the mammalian Doublesex homolog DMRT1 in the juvenile testis. *Proceedings of the National Academy of Sciences of the United States of America* **107**, 13360–13365 (2010).

39. Gartland, A. *et al.* In vitro chondrocyte differentiation using costochondral chondrocytes as a source of primary rat chondrocyte cultures: an improved isolation and cryopreservation method. *Bone* **37**, 530–544 (2005).

40. Ge, S.X., Son, E.W. & Yao, R. iDEP: an integrated web application for differential expression and pathway analysis of RNA-Seq data. *BMC Bioinformatics* **19**, 534 (2018).

41. Yoshida, M. *et al.* The transcription factor Foxc1 is necessary for Ihh-Gli2-regulated endochondral ossification. *Nature communications* **6**, 6653 (2015).

# Figures
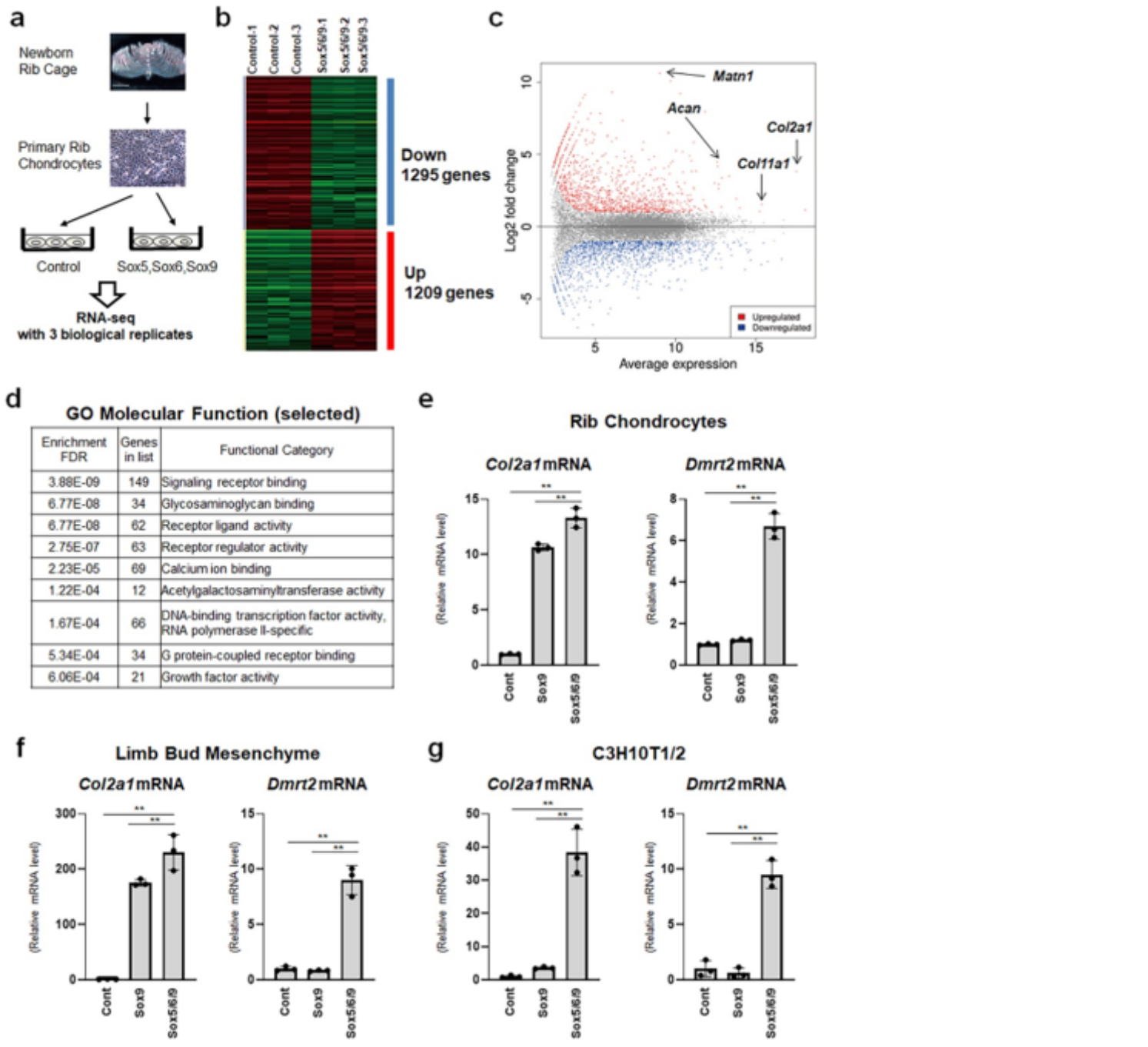
**Figure 1**

Identification of Dmrt2 as a downstream transcription factor of Sox5/6/9. (a) Schematic model of RNA-seq analysis using newborn mouse rib chondrocytes with adenovirus-mediated overexpression of Sox5, Sox6, and Sox9. (b) Expression patterns of differentially expressed genes (DEGs). (c) MA plot analysis of DEGs. (d) Classification analysis of upregulated genes with GO molecular function. Selected molecular functions from Supplemental Data 1 are shown. (e–g) Total RNA was isolated from primary chondrocytes (e), limb bud mesenchyme from E12.5 mouse limb buds (f), and C3H10T1/2 cells (g) infected with control (Cont), Sox9 (Sox9), or Sox5+Sox6+Sox9 (Sox5/6/9) adenoviruses. Col2a1 and Dmrt2 mRNA expression levels were analyzed by RT-qPCR. The RNA level is indicated as the fold increase

compared with that of the control. Data are shown as the mean ± s.d. (n = 3). **p < 0.01; one-way analysis of variance (ANOVA) followed by the Tukey test.
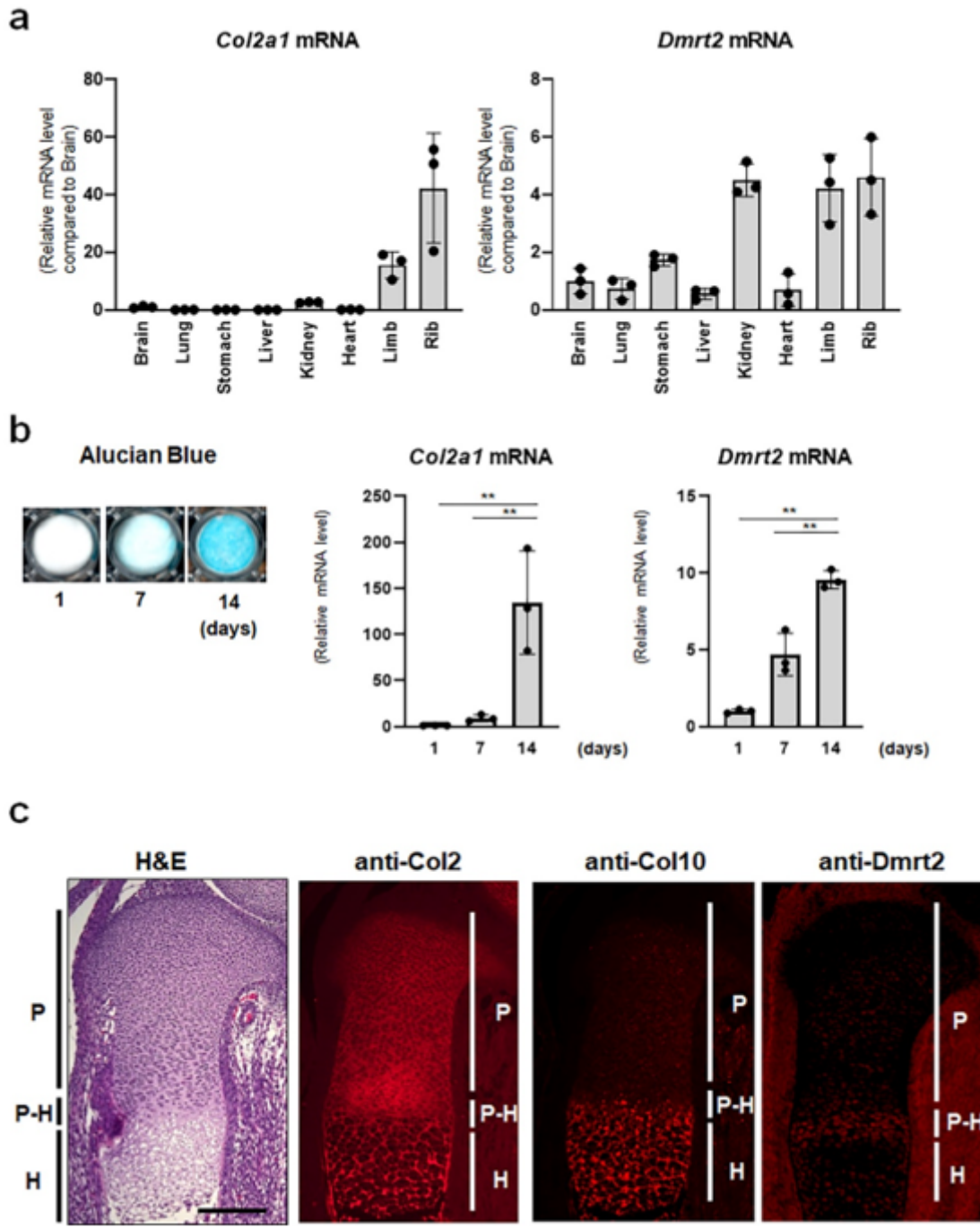


## Figure 2

Expression of Dmrt2 in chondrocytes. (a) Tissue distribution of Dmrt2 and Col2a1 mRNAs in newborn mouse tissues. Total RNA was isolated from the indicated tissues of newborn mice and analyzed by RT-qPCR. The relative mRNA expression compared with that in brain is indicated, with the expression level in brain set as 1. Data are shown as the mean ± s.d. (n = 3). (b) ATDC5 cells were cultured in the presence of insulin-transferrin-selenium (ITS) for the indicated time and then stained with Alcian blue (left panel). Total RNA isolated from these cells was analyzed by RT-qPCR for Col2a1 (middle panel) and Dmrt2

expression (right panel). The RNA level is indicated as the fold increase compared with that on day 1. Data are shown as the mean ± s.d. (n = 3). **p < 0.01 (vs. day 1); one-way analysis of variance (ANOVA) followed by the Tukey test. (c) Immunohistochemical analysis of Dmrt2 in growth plate chondrocytes. Sections of an E15.5 mouse tibia were subjected to H&E staining and immunocytochemical analyses using anti-Col2, -Col10, and -Dmrt2 antibodies. Scale bar: 200 μm. P: proliferating chondrocytes; P-H: pre-hypertrophic chondrocytes; H: hypertrophic chondrocytes.
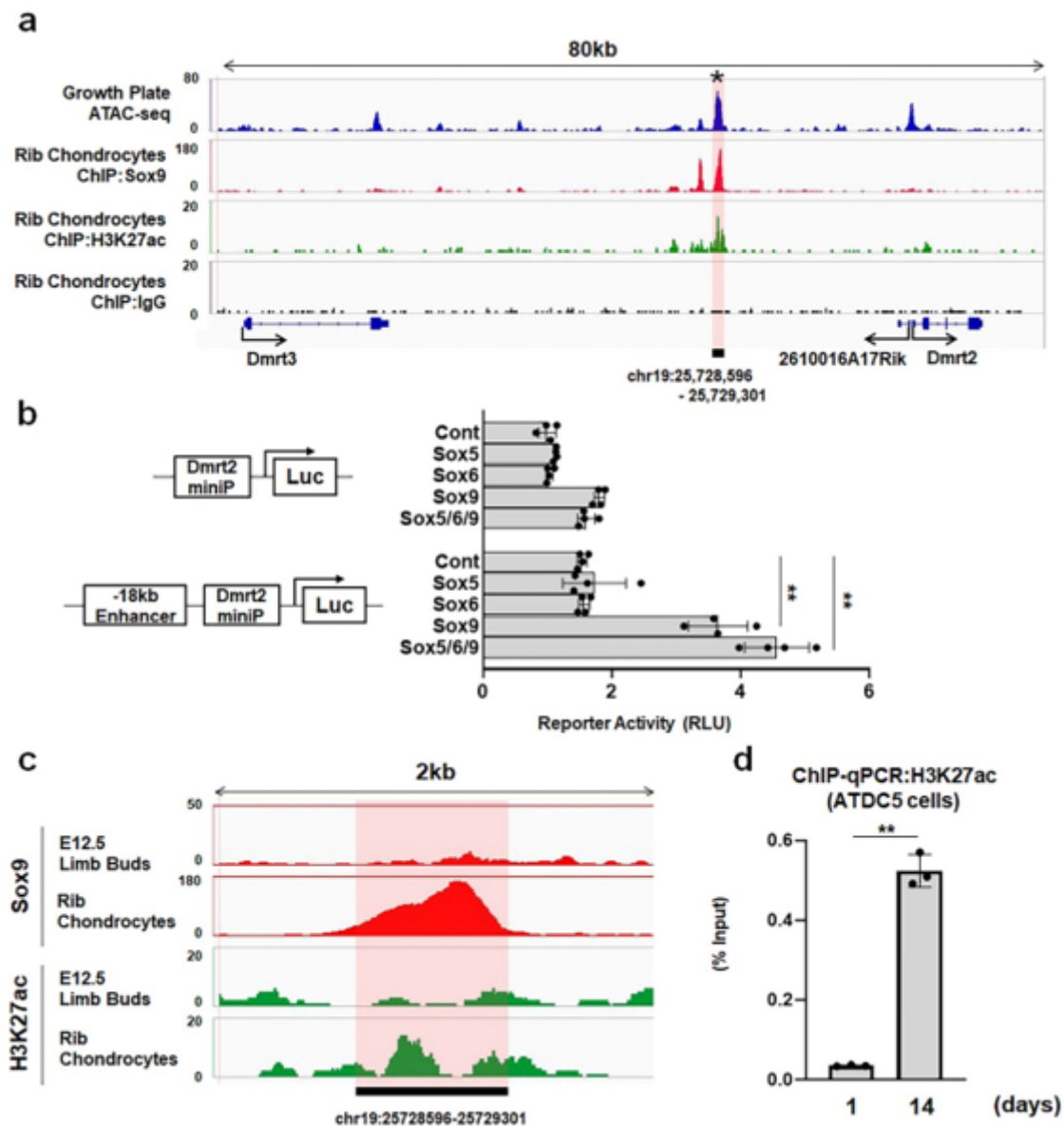


Figure 3

Epigenetic regulation of Dmrt2 gene expression in chondrocytes (a) ATAC-seq profiles of growth plate chondrocytes (GSE100585) and ChIP-seq profiles of primary newborn rib chondrocytes for Sox9, H3K27ac, and IgG (GSE69109) at Dmrt2 gene loci. Note that strong ATAC-seq peaks overlapped with ChIP-seq peaks for Sox9 and H3K27ac. (b) HEK293 cells were transfected with reporter plasmids together with or without Sox9-bound enhancer and Sox5/6/9 as indicated. Luciferase activities were measured at 48 h after transfection. Data are shown as the mean ± s.d. (n = 4). **p < 0.01 (vs. Control); one-way

ANOVA followed by the Tukey test. (c) ChIP-seq profiles for Sox9 (GSE73225) and H3K27ac (GSE45456) in E12.5 limb buds and newborn primary rib chondrocytes (GSE69109). (d) ChIP-qPCR analysis for Sox9-bound enhancer of the Dmrt2 gene using anti-H3K27ac antibody in ATDC5 cells. Data are shown as the mean ± s.d. (n = 3). **$p < 0.01$ (vs. day 1); Student's t-test.
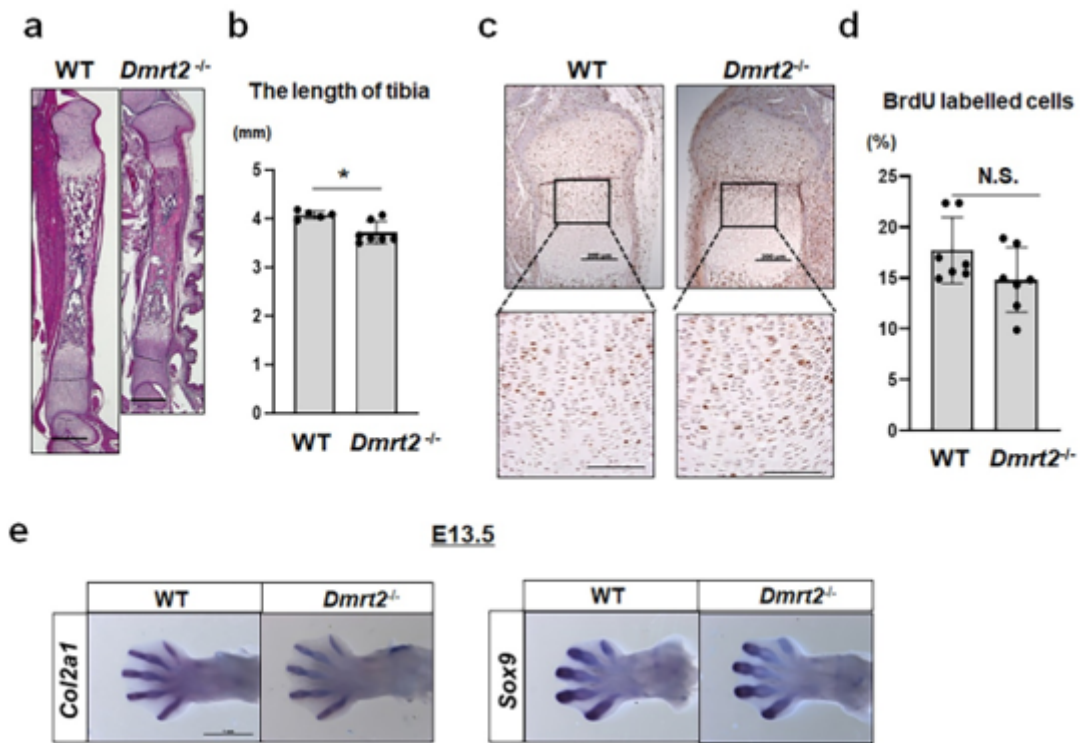


**Figure 4**

Dwarfism phenotype in Dmrt2▯/▯ mice. (a) Sections of tibiae from newborn WT and Dmrt2▯/▯ littermate mice were examined by hematoxylin and eosin (H&E) staining. Scale bar: 500 μm. (b) Quantitative analysis of tibia lengths in newborn WT and Dmrt2▯/¬▯ mice. Data are shown as the mean ± s.d. (WT; n = 5, Dmrt2▯/¬▯; n = 7). *$p < 0.05$ (vs. WT); Student's t-test. (c, d) BrdU labelling assay of WT and Dmrt2▯/▯ littermate mice. (c) Representative images of BrdU staining. Scale bars, 200 μm (upper panel) and 100 μm (lower panel). (d) Quantitative analysis of the proliferation rate of columnar chondrocytes. The ratio of BrdU-positive nuclei to total hematoxylin-positive nuclei was calculated. BrdU-positive nuclei in round-resting and hypertrophic chondrocytes were excluded from the analysis. Data are shown as the mean ± s.d. (n = 6). N.S., not significant. (e) Whole-mount in situ analysis of Col2a1 and Sox9 in hindlimbs from E13.5 WT and Dmrt2▯/▯ littermate embryos. Scale bar: 1 mm.
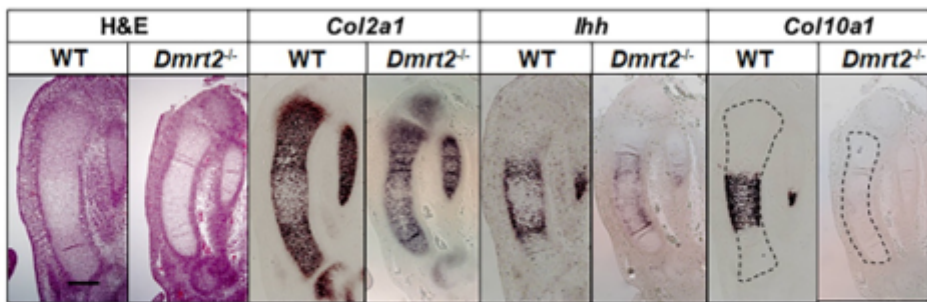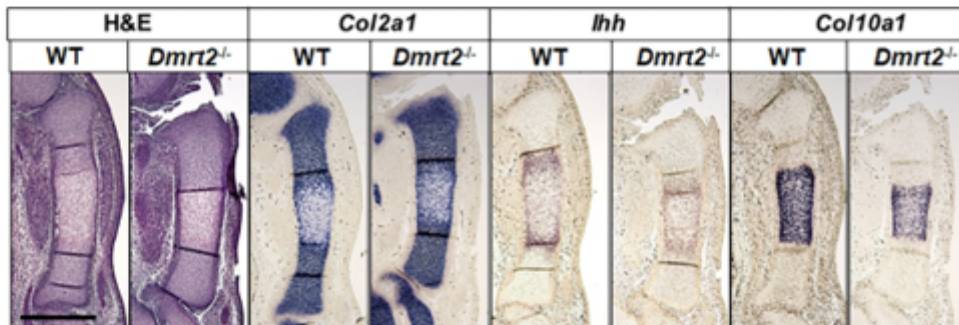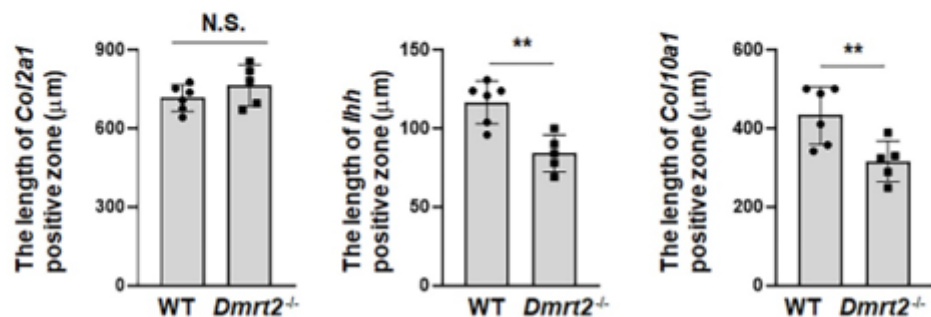
**Figure 5**

Delayed onset of chondrocyte hypertrophy in Dmrt2⬚/⬚ mice. (a, b) Sections of tibiae from E14.5 (a) and E15.0 (b) WT and Dmrt2⬚/⬚ littermate embryos were examined by hematoxylin and eosin (H&E) staining and RNA in situ hybridization analysis using antisense probes against Col2a1, Ihh, and Col10a1. Scale bars: 200 μm (E14.5), 500 μm (E15.0). (c) Quantitative analysis of Col2a1-positive length, Ihh-positive length, and Col10a1-positive length in E15.0 WT and Dmrt2⬚/⬚ mice. Data are shown as the mean ± s.d. (WT; n = 6, Dmrt2⬚/¬⬚; n = 5). *p < 0.05 (vs. WT); Student's t-test.
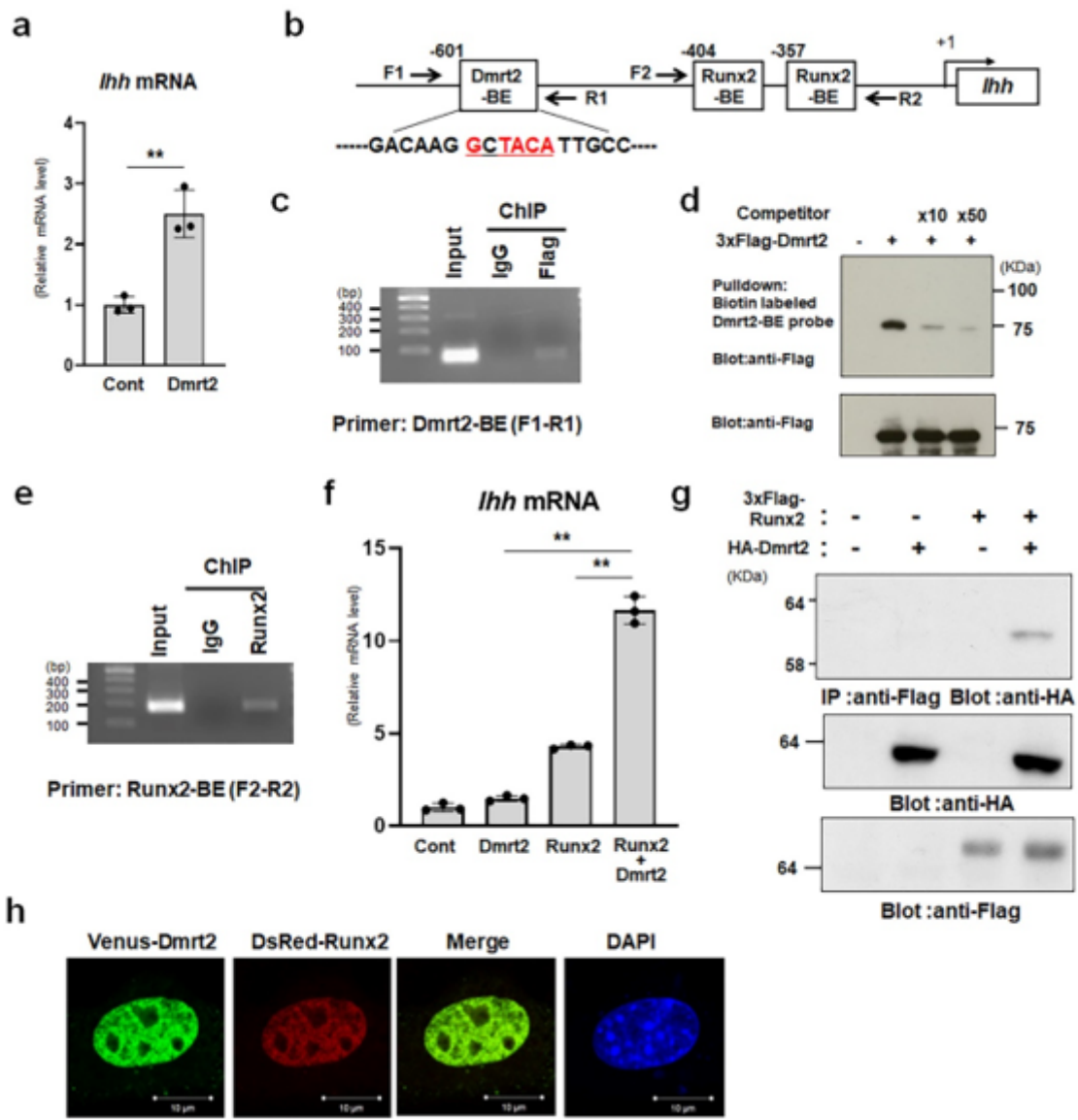
**Figure 6**

Dmrt2 promotes Ihh expression in collaboration with Runx2. (a) Primary chondrocytes were infected with the control (Cont) or Flag-tagged-Dmrt2 adenovirus, and Ihh expression was analyzed by RT-qPCR. Data are shown as fold changes normalized to Cont (mean ± s.d.) (n = 3). **p < 0.01 (vs. WT); Student's t-test. (b) Schematic representation of the putative Dmrt2-binding element (-BE) (GnTACA) in the mouse Ihh gene promoter. (c) ChIP assay using normal IgG and anti-Flag antibody. Binding of Flag-Dmrt2 to the Ihh gene promoter in primary chondrocytes was examined by PCR. (d) DNA pull-down assays using the Dmrt2-binding element in the mouse Ihh gene promoter. Samples precipitated with a biotin-labeled Dmrt2-BE oligonucleotide (upper panel) and cell lysates (lower panel) were examined by immunoblotting with an anti-Flag antibody. (e) ChIP assays using normal IgG and anti-Runx2 antibody. Binding of Runx2 to the Ihh gene promoter in primary chondrocytes was examined by PCR. (f) Dmrt2 and Runx2 synergize to induce Ihh mRNA expression in primary chondrocytes. The RNA level is indicated as the fold increase compared with the level in the control. Data are shown as the mean ± s.d. (n = 3). **p < 0.01; one-way ANOVA followed by the Tukey test. (g) Dmrt2 physically associates with Runx2. Cell lysates were

immunoprecipitated with anti-Flag antibody and then immunoblotted with anti-HA antibody (top). Cell lysates were immunoblotted with anti-HA (middle) or anti-Flag (bottom) antibodies. (h) Colocalization of Dmrt2 and Runx2 in the nucleus. C3H10T1/2 cells were transfected with both Venus-tagged-Dmrt2 (Venus-Dmrt2) and DsRed-tagged-Runx2 (DsRed-Runx2). Confocal sections were visualized under a fluorescence microscope. Scale bar: 10 μm.
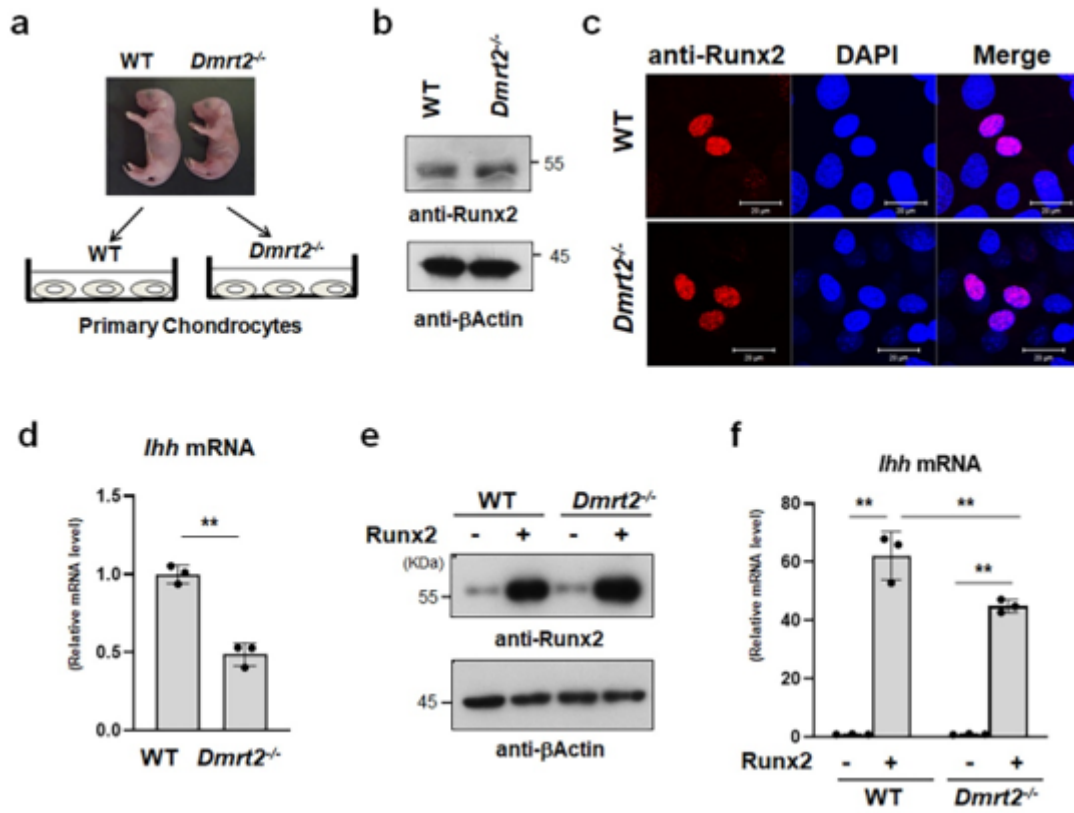


## Figure 7

Impaired Runx2 function in Dmrt2−/▢ chondrocytes. (a) The method to examine the effects of Runx2 and Sox9 in WT and Dmrt2▢/▢ chondrocytes. (b) Primary chondrocytes were isolated from newborn WT and Dmrt2▢/▢ littermate mice and cultured for 3 days. Cell lysates were analyzed by immunoblotting with anti-Runx2 and anti-▢-actin antibodies. (c) Nuclear localization of Runx2 in primary chondrocytes of WT and Dmrt2▢/▢ chondrocytes. Confocal sections were visualized under a fluorescence microscope. Scale bar: 20 μm. (d) Total RNA was isolated from primary chondrocytes of WT and Dmrt2▢/▢ littermate mice, and then Ihh mRNA expression was determined by RT-qPCR. Data are shown as fold changes normalized to WT (mean ± s.d., n = 3). **p < 0.01 (vs. WT); Student's t-test. (e) Primary chondrocytes from WT and Dmrt2▢/▢ littermate mice were infected with Runx2 adenovirus and cultured for 4 days. Cell lysates were analyzed using immunoblotting with anti-Runx2 and anti-▢-actin antibodies. (f) Primary chondrocytes from WT and Dmrt2▢/▢ littermate mice were infected with the control (▢) or Runx2 adenovirus and then cultured for 4 days. Total RNA was isolated and Ihh mRNA expression was determined by RT-qPCR. The RNA level is indicated as the fold increase compared with that of the WT control. **p < 0.01; one-way ANOVA followed by the Tukey test.

# Supplementary Files

This is a list of supplementary files associated with this preprint. Click to download.

- Dmrt2SIOnoComBiol0820.pdf